Korean J. Chem. Eng., **17**(2), 169-173 (2000)

Experimental Studies on the Instabilities of Viscous Fingering in a Hele-Shaw Cell

Chung Gi Baig, Young Ho Chun*, Eun Su Cho* and Chang Kyun Choi†

School of Chemical Engineering, Seoul National University, Seoul 151-742, Korea
*R&D Center, Kumho Chemicals, Inc., Kyunggi-do 467-810, Korea
(*Received 15 June 1999 • accepted 12 January 2000*)

Abstract−When air is injected into silicone oil contained in a horizontal Hele-Shaw cell, a single air bubble forms and grows showing various interesting phenomena. In this study the effects of the bubble front velocity, air injection velocity at a nozzle, fluid properties and cell depth on the stability of the growing bubble were investigated experimentally. By using the modified capillary number involving the aspect ratio, we obtained the onset conditions of the unstable bubble. Also, the bubble width was analyzed both quantitatively and qualitatively. Before the bubble experiences splitting, the bubble front velocity is almost proportional to the air injection velocity. Therefore the latter velocity may be used in a practical sense.

Key words: Air Injection Velocity, Bubble Front Velocity, Bubble Width, Capillary Number, Hele-Shaw Cell

INTRODUCTION

When a less viscous fluid penetrates into a more viscous fluid, the interface can become unstable. With the unstable interface formed the flow behavior is very much complicated and intriguing. Therefore, many studies on viscous fingering have been conducted with a Hele-Shaw cell, as shown in Fig. 1, which consists of two parallel plates with a narrow space. As air penetrates into the liquid filling the cell, the resulting two-phase flow is two-dimensional. With time, the initial flat interface becomes wavy and fingers appear.

For a simple, stable finger Saffman and Taylor [1958] obtained a solution describing the shape of the stable bubble by neglecting the surface tension effect. McLean and Saffman [1981] performed a numerical analysis of the bubble shape by including the surface tension effect and proposed that the most important parameter is the modified capillary number Ca_m defined as

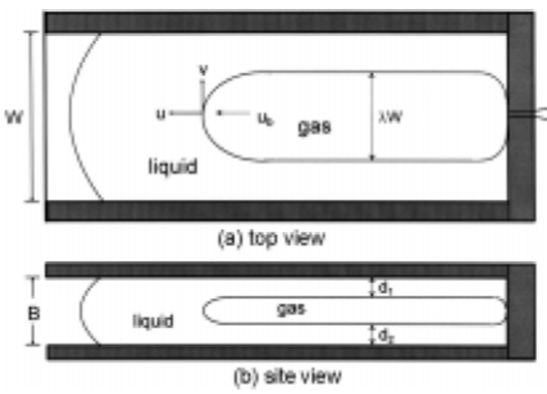

Fig. 1. Schematic diagram of stable bubble growing in present Hele-Shaw cell.

†To whom correspondence should be addressed.
E-mail: ckchoi@snu.ac.kr

$$Ca_m=12Ca(W/B)^2 \quad (1)$$

where Ca (=μu/γ) is the capillary number. μ, u, γ, W and B denote the liquid viscosity, the bubble front velocity, the surface tension, the cell width, and the cell depth, respectively. λ, the bubble width nondimensionalized by W, is closely related with Ca_m. Tabeling et al. [1987] examined experimentally the relation between λ and Ca_m, and reported that in the range of $Ca_m \leq 5$ the dimensionless bubble width λ decreases with increasing Ca_m, showing a linear relation.

With increasing Ca_m the advancing interface becomes unstable. Bensimon [1986] reported that the amplitude of the noise existing along the interface increases exponentially as a function of Ca_m. The bubble growth with three-step mechanism of shielding, spreading, and splitting is well illustrated by Homsy [1987]. Cho et al. [1997] reported bubble instabilities resulting in branches developed by splitting and the onset position of instability. They conducted experiments by using viscous silicone oils of μ/ρ=1, 10^2 and 10^3 St. Here their work is complemented by using less-viscous silicone oils. The critical condition of onset of instability exhibiting the inflection point or splitting is obtained as a function of the modified capillary number. In particular, the gas velocity through the inlet nozzle is shown to be almost proportional to the front velocity of the bubble before it splits. Therefore, its use as the characteristic velocity is tested here.

SYSTEM DESCRIPTION

The system considered here is illustrated in Fig. 1. A horizontal Hele-Shaw cell of width W and depth B is filled initially with liquid. At time t=0 inert gas is injected into the liquid in the cell with the air injection velocity u_n at the nozzle. The bubble with the growth velocity u_n grows with the front velocity u_b under stable conditions. In this system the important parameters are

(capillary number) $\quad Ca=\mu u/\gamma \quad (2)$

(dimensionless bubble width) λ=[bubble width]/[cell width] (3)

(modified capillary number) $Ca_m = (12\mu u_b/\gamma)(W/B)^2$ (1)

$$\overline{Ca}_m = (12\mu u_n/\gamma)(W/B)^2 \quad (4)$$

where γ denotes the surface tension.

For small B the flow behavior follows Darcy's law and the factor of $B^2/12$ corresponds to the permeability in a porous layer. Saffman and Taylor [1958] showed that the position of a bubble surface follows on the two-dimensional horizontal plane:

$$x = \frac{(1-\lambda)W}{2\pi} \ln\frac{1}{2}\left[1 + \cos\left(\frac{2\pi y}{\lambda W}\right)\right] \quad (5)$$

which agrees well with the stable finger of negligible surface tension. Here x and y denote the symmetric interface position of a growing bubble. The thickness of liquid film left behind a bubble (see d_1 and d_2 in Fig. 1) is decided by Ca and B [Tabeling et al., 1987; Cho et al., 1997]. For large Ca the bubble does not grow into the stable finger illustrated above. It has been known that the bubble is destabilized at $Ca_m \cong 900$-7000. Cho et al. [1997] reported that there appears a finger having branches on one side [see Park and Homsy, 1985] for $900 < Ca_m < 4000$ and the finger showing tip-splitting at $Ca_m \cong 4000$, and with higher Ca_m-values flow patterns become more complicated by increasing the number of lobes. The splitting behavior is known to be the interplay of shielding and spreading. Since the incipient instabilities produce different interface shapes depending on the capillary number, the present experiments concentrated on the finger behavior for $Ca_m < 3000$.

EXPERIMENTS

The schematic diagram of the present experimental apparatus is presented in Fig. 2. The cell was composed of the bottom and the lateral sides of metal, and the flows were observed through the top transparent acrylic plate. Several clamps were fixed at the edge of the cell with a constant interval for preventing fluid from leaking out to the lateral gap. The width and length of the cell are fixed at 10 cm and 50 cm, respectively. The cell depths were fixed at 2, 3 and 5 mm, respectively. Five different kinds of silicone oils (50, 100, 350, 500 and 1000 cSt) were used. Their densities were almost the same as water. Temperature was maintained at 25 °C by using a temperature controller. After the cell was filled with silicone oil, air was injected into the oil through a small hole of 1.2 mm diameter by a syringe pump. The gas flow rate was controlled within the range of 0.51-27.2 ml/min. The viscosity of silicone oil, which is a crucial factor in bubble growth, was measured by a viscometer (Rheometrics, RMS-800E). After injection, the bubble propagation was photographed by a video camera installed above the cell and the films were analyzed by using a computer.

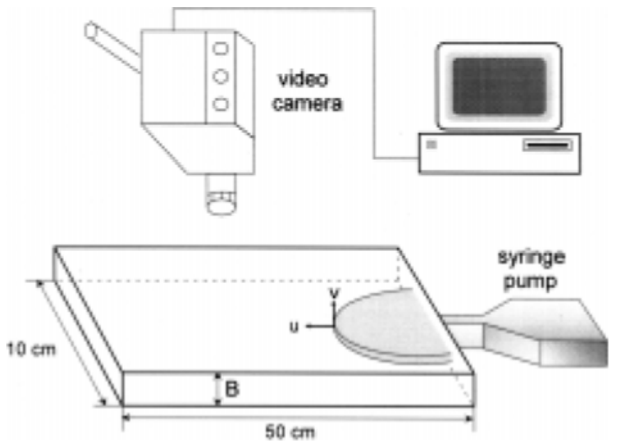

Fig. 2. Schematic diagram of experimental apparatus.

RESULTS AND DISCUSSION

A bubble is formed when air is injected into silicone oil through a nozzle. The bubble grows and its shape is determined depending on the magnitude of velocities and fluid properties. In the present experiments three types of shapes of the bubble interface were observed at the early stage of bubble growth: (a) stable, (b) marginally stable, and (c) unstable ones, as shown in Fig. 3. Here are classified bubbles of (b) and (c) as Type I [Fig. 3(b)] and Type II [Fig. 3(c)], respectively. The primary object of this study is to find the conditions for exhibiting the interface shapes of Type I and Type II.

A stable bubble shows initially a rounded interface like a semicircle, as is shown in Fig. 3(a), and grows into a finger, whose interface is well approximated by Eq. (5). The effect of surface ten-

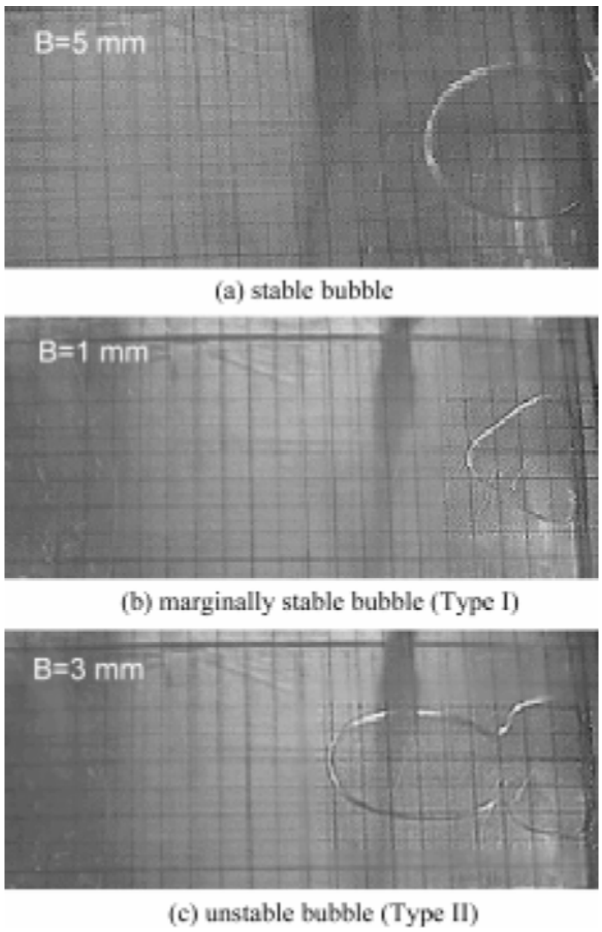

Fig. 3. Three kinds of bubbles at their early stages of growth.

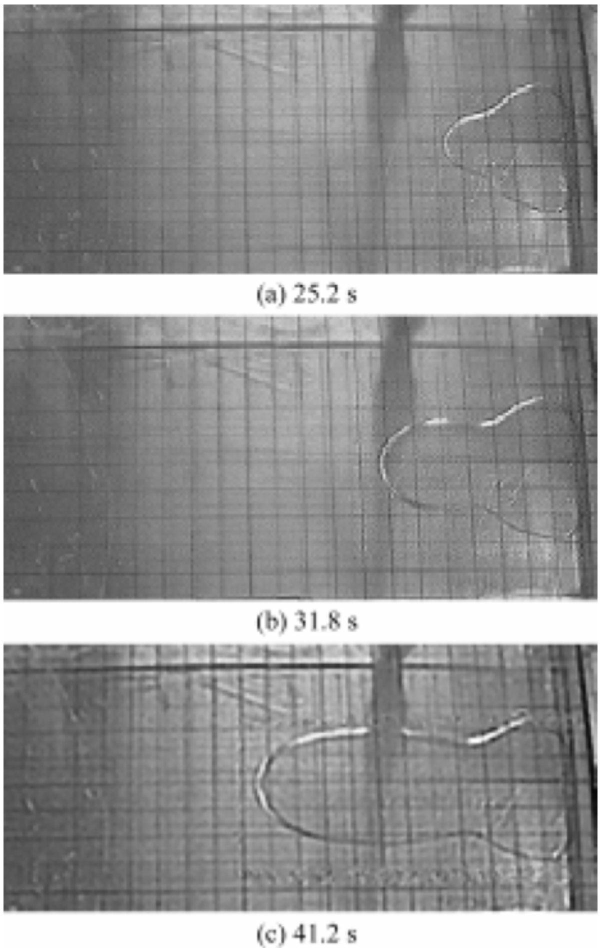

Fig. 4. Bubble propagation of Type I with time for B=2 mm, μ =0.490 Pa s and u_n=19.2 cm/s.

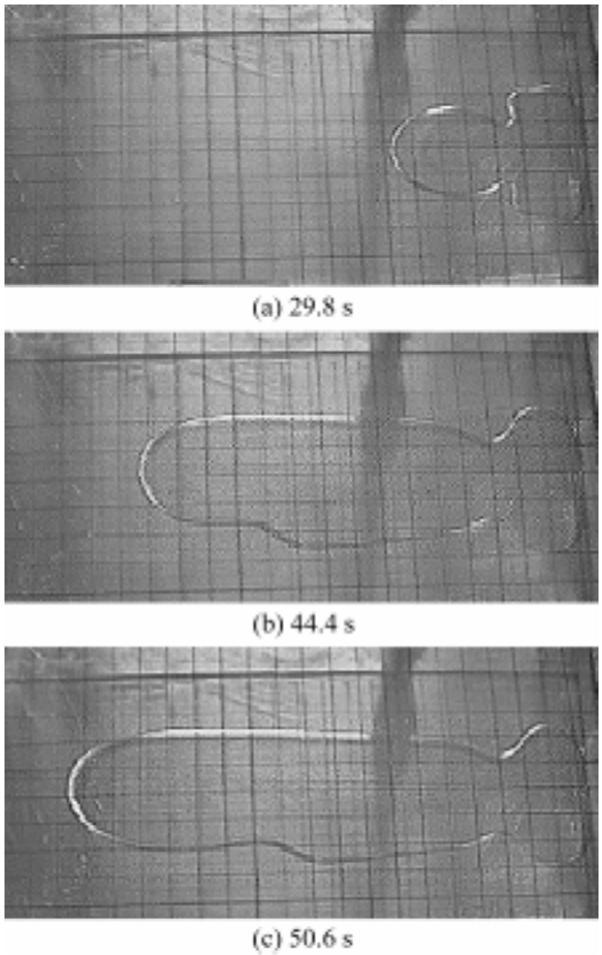

Fig. 5. Bubble propagation of Type II with time for B=2 mm, μ =0.969 Pa s and u_n=40.1 cm/s.

sion flattens the finger front to a certain degree [Cho, 1996]. The finger tip grows fastest because the distance between the bubble front and the liquid front is the shortest. With time the bubble width becomes constant for each experimental run of stable fingers.

A marginally stable bubble is illustrated with time in Fig. 4. This bubble becomes more stable with time and finally produces a stable finger. As shown in the figure, its initial shape is a kind of triangle far from a semi-circle, that is thought to be the result of weak instabilities. These Type-I instabilities may be called the prelude of unstable fingers. As perturbations increase, Type I develops into Type II. Type-II instabilities bring tip splitting and branches, as are shown in Fig. 5, which do not follow Eq. (5). It has been observed that splitting behaviors have periodicity with growth.

In the present experiments of $3.77 \leq Ca_m \leq 7.37 \times 10^3$ it was found that there appear Type I for $800 \leq Ca_m < 2000$ and Type II for $Ca_m \geq 2000$. These values are comparable with those of other reports [Park and Homsy, 1985; Tabeling et al., 1987; DeGregoria and Schwartz, 1985; Cho et al., 1997]. Therefore it may be stated that the finger is stable for $Ca_m < 800$.

The bubble width measured here is compared with other existing results in Fig. 6. The present λ-values were obtained from the photos of fingers, which agree favorably with Tabeling et al.'s [1987]. In obtaining λ-values bubbles exhibiting splitting were excluded. Because Cho et al. [1997] used very viscous silicone oils

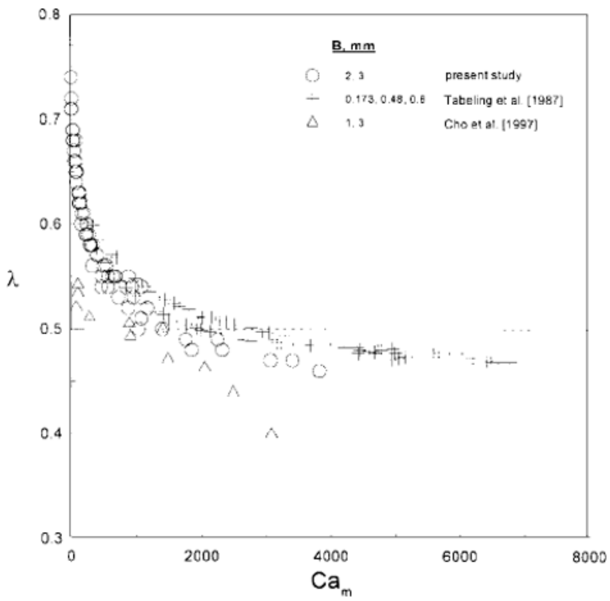

Fig. 6. Comparison of present data of λ vs. Ca_m with those of Tabeling et al. [1987] and Cho et al. [1997].

of 1-10^3 St, their λ-values may be lower than other results. Saffman and Taylor [1958] reported that with an increase in Ca_m, λ

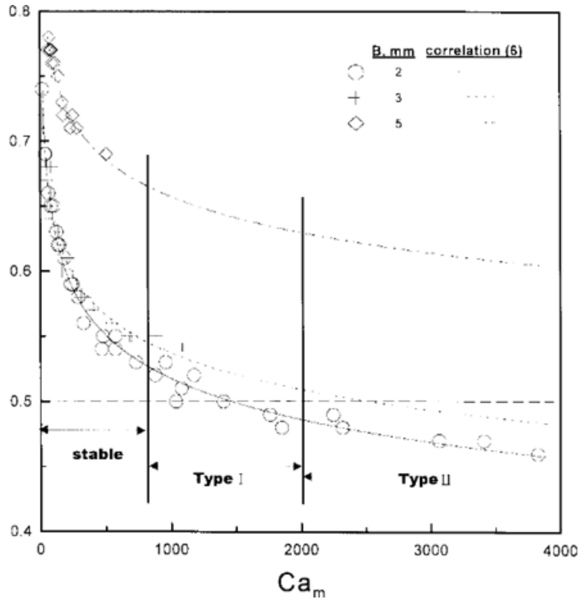

Fig. 7. λ vs. Ca_m with apparently stable fingers growing.

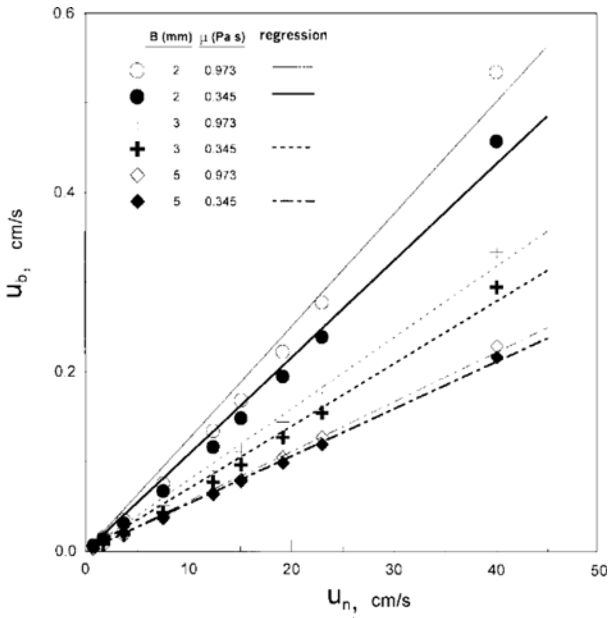

Fig. 8. u_b vs. u_n with silicone oils of μ=0.345 and 0.973 Pa s for each cell depth.

is close to 1/2 unless the flow is very slow. Considering stable fingers of Ca_m<800, this limiting λ-value seems reasonable. Fingers of Ca_m≥800 may be potentially unstable. In other words, there is a possibility of their split at a very large position. The present results of λ-values are summarized in Fig. 7. They showed the following nonlinear relation between λ and Ca_m:

$$\lambda=\alpha Ca_m^{\beta} \tag{6}$$

where α and β are empirical constants. The correlation resulted in α=0.960, β=−0.0895 for B=2 mm and α=0.909, β=−0.0763 for B=3 mm, and α=1.005, β=−0.0615 for B=5 mm. Thus, for a given Ca_m the λ-value decreases with a decrease in depth B, but it approaches an asymptote for B≤2 mm. It seems evident that the gravitational force by the liquid film on the boundaries affects the bubble behavior [Maxworthy, 1987]. Park et al. [1994] reported that for the Bond number ($=\rho g B^2/\gamma$) Bo>1.5 a gravity effect may exist. Here ρ denotes the liquid density and g the gravitational acceleration. Since in the present experiments Bo=1.8 for B=2 mm, Bo=4.1 for B=3 mm and Bo=11.3 for B=5 mm, λ increases with an increase in B, as shown in Fig. 7. Cho et al. [1997] reported that splitting occurs later with an increase in B for B=1-3 mm. In this B-range it is supposed that Bo is the measure of stabilization. But for B=5 mm the buoyancy force exhibited by the bubble itself may be significant. It is mentioned that the case of B≤2 mm follows the conventional Hele-Shaw equations.

From a practical viewpoint it will be more convenient to use the air injection velocity u_n at the nozzle instead of the finger-tip velocity u_b, for u_b is not easily measured. The experimental results showed that u_n and u_b have a linear relation, as shown in Fig. 8. Therefore $\overline{Ca}_m$ defined by Eq. (4) may be used instead of Ca_m. In the present system the bubble was stable for $\overline{Ca}_m$<8.0×10^4. It was observed that with decreasing μ and increasing B, the slope decreases. For the same inlet flow rate, a decrease in μ and an increase in B bring an increase in both the bubble width and the liquid film thickness. This results in decreasing u_b relatively. Here

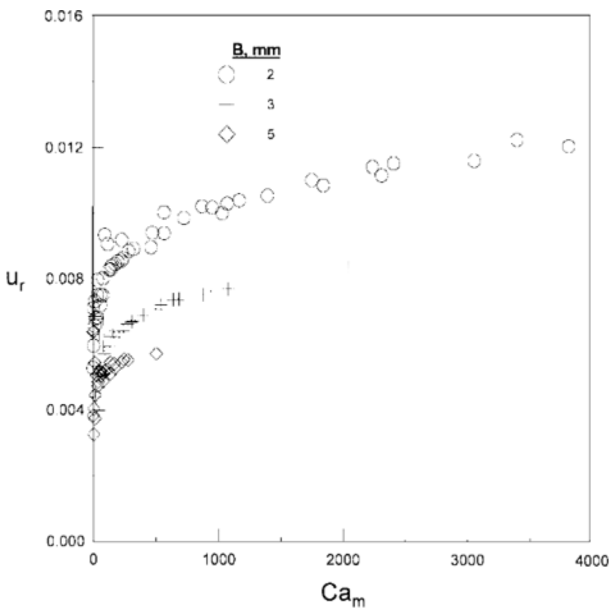

Fig. 9. Comparison of u_r-values among three cell depths with calculated Ca_m-values.

the relative velocity u_r ($=u_b/u_n$) is introduced. It may be supposed that the larger u_r-value is, the more the possibility of instability exists. Fig. 9 shows that for a given Ca_m, u_r increases with decreasing cell depth B. As mentioned before, the λ-values are different for each cell depth if the gravitational effect by the liquid film is significant. The relative velocity u_r itself includes the gravity effect caused by an increase in cell depth. In this connection further study is required.

CONCLUSIONS

In the present study bubble instabilities were investigated experimentally in a Hele-Shaw cell of B=2, 3 and 5 mm and they were categorized here as two types, Type I and Type II. Type I appears for $800 \le Ca_m < 2000$ and Type II for $Ca_m \ge 2000$. Also, it was observed that λ-values decrease below 1/2 for $Ca_m > 1500$. In the present experimental range the gravity effect due to the liquid film stabilized the system and increased the bubble width. The relative velocity u_r increased with a decrease in B but with an increase in Ca_m.

ACKNOWLEDGEMENTS

The authors wish to thank the R&D Center, Kumho Chemicals, Inc., Seoul for the financial support of this work.

NOMENCLATURE

B : cell depth [m]
Ca : capillary number [$\mu u/\gamma$]
Ca_m : modified capillary number, $(12\mu u_b/\gamma)(W/B)^2$
$\overline{Ca}_m$: modified capillary number with nozzle velocity, $(12\mu u_n/\gamma)(W/B)^2$
d_1, d_2 : upper or lower thickness of liquid film [m]
g : gravitational acceleration [m/s^2]
t : time [s]
u : bubble velocity in length direction [m/s]
u_b : bubble velocity [m/s]
u_n : air injection velocity at inlet nozzle [m/s]
u_r : relative velocity, u_b/u_n [-]
v : bubble velocity in spanwise direction [m/s]
W : cell width [m]
x, y : position of bubble interface [-]

Greek Letters

γ : surface tension [N/m]
λ : dimensionless bubble width [-]
μ : viscosity [Pa s]
ρ : density [Kg/m^3]

REFERENCES

Bensimon, D., "Stability of Viscous Fingering," *Phys. Rev. A*, **33**, 1302 (1986).

Cho, E. S., "An Experimental Study on Two-phase Flow Characteristics in Gas-injected Hele-Shaw Cells," Ph.D. Thesis, Seoul National University, Seoul (1996).

Cho, E. S., Yoon, D.-Y., Choi, C. K. and Hwang, I. G., "Experimental Studies on Gas-injected Finger Convection in a Hele-Shaw Cell," Proc. 4th World Conf. Experimental Heat Transfer, Fluid Mech. and Thermodynamics, Edizioni ETS, Pisa, **4**, 2143 (1997).

DeGregoria, A. J. and Schwartz, L. W., "Finger Break-up in Hele-Shaw Cells," *Phys. Fluids*, **28**, 2312 (1985).

Homsy, G. M., "Viscous Fingering in Porous Media," *Ann. Rev. Fluid Mech.*, **19**, 271 (1987).

Maxworthy, T., "The Nonlinear Growth of a Gravitationally Unstable Interface in a Hele-Shaw Cell," *J. Fluid Mech.*, **177**, 297 (1987).

McLean, J. W. and Saffman, P. G., "The Effect of Surface Tension on the Shape of Fingers in a Hele-Shaw Cell," *J. Fluid Mech.*, **102**, 455 (1981).

Park, C.-W. and Homsy, G. M., "The Instability of Long Fingers in Hele-Shaw Flows," *Phys. Fluids*, **28**, 1583 (1985).

Park, C.-W., Marurada, S. R. and Yoon, D.-Y., "The Influence of Surfactant on the Bubble Motion in Hele-Shaw Cells," *Phys. Fluids*, **6**, 3267 (1994).

Saffman, P. G. and Taylor, G. I., "The Penetration of a Fluid into a Porous Medium Hele-Shaw Cell Containing a More Viscous Liquid," Proc. Royal Soc. Lond. A, **245**, 312 (1958).

Tabeling, P., Zocchi, G. and Libchaber, A., "An Experimental Study of the Saffman-Taylor Instability," *J. Fluid Mech.*, **177**, 67 (1987).